Stratospheric ozone depletion inside the volcanic plume shortly after the 2022 Hunga Tonga eruption

Yunqian Zhu[1,2,3], Robert W. Portmann[1], Douglas Kinnison[4], Owen Brian Toon[3,5], Luis Millán[6], Jun Zhang[4], Holger Vömel[7], Simone Tilmes[4], Charles G. Bardeen[4], Xinyue Wang[4], Stephanie Evan[8], William J. Randel[4], Karen H. Rosenlof[1]

1. NOAA, Chemical Sciences Laboratory
2. Cooperative Institute for Research in Environmental Sciences, University of Colorado Boulder
3. Laboratory for Atmospheric and Space Physics, University of Colorado Boulder
4. NCAR, Atmospheric Chemistry Observations and Modeling Laboratory
5. Department of Atmospheric and Oceanic Sciences, University of Colorado Boulder
6. Jet Propulsion Laboratory, California Institute of Technology, 4800 Oak Grove Drive, Pasadena, CA 91109, USA
7. NCAR, Earth Observing Laboratory
8. Laboratoire de l'Atmosphère et des Cyclones (LACy, UMR8105, CNRS, Université de La Réunion, Météo-France), Saint-Denis, France

Corresponding author: Yunqian Zhu (yunqian.zhu@noaa.gov)

Abstract

Near-term in-plume ozone depletion was observed for about ten days by Microwave Limb Sounder (Aura/MLS) right after the January 2022 Hunga Tonga-Hunga Ha'apai (HTHH) eruption. This work analyzes the dynamic and chemical causes of this ozone depletion. The results show that the large water injection (~150 Tg) from the HTHH eruption, with ~0.0013 Tg injection of ClO (or ~0.0009 Tg of HCl), causes ozone loss due to strongly enhanced HOx and ClOx cycles and their interactions. Aside from the gas phase chemistry, the heterogeneous reaction rate for $HOCl+HCl\rightarrow Cl_2+H_2O$ increases to 10^4 $cm^{-3}sec^{-1}$ and is a major cause of chlorine activation, making this event unique compared with the springtime polar ozone depletion where $HCl+ClONO_2$ is more important. The large water injection causes relative humidity over ice to increase to 70% - 100%, decreases the H_2SO_4/H_2O binary solution weight percent to 35% compared with the 70% ambient value, and decreases the plume temperature by 2-6 K. These changes lead to high heterogeneous reaction rates. Plume lofting of ozone-poor air is evident during the first two days after the eruption, but ozone concentrations quickly recover because its chemical lifetime is short at 20 hPa. With such a large seawater injection, we expect that ~5 Tg Cl was lifted into the stratosphere by the HTHH eruption in the form of NaCl, but only ~0.02% of that remained as active chlorine in the stratosphere. Lightning NOx changes are probably not the reason for the HTHH initial in-plume O_3 loss.

Key points:
- HOCl is identified as playing a large role in the in-plume chlorine balance and heterogeneous processes, making this event unique compared with the ozone hole where $HCl+ClONO_2$ is more important.
- The HTHH eruption enhanced the HOx/ClOx cycles and their interactions, which caused in-plume O_3 depletion.

Deleted: In

Deleted: lightning

49   ● The injection of Cl, H₂O, and lightning NOx modified the ambient chemistry.
50
51   **1. Introduction**
52   Stratospheric ozone concentrations change after volcanic eruptions for a variety of reasons.
53   Enhanced polar ozone depletion occurs after large or medium volcanic eruptions [*Hofmann and*
54   *Oltmans*, 1993; *Portmann et al.*, 1996; *Solomon et al.*, 2016] since heterogeneous reactions on
55   volcanically enhanced sulfate aerosols result in amplified anthropogenic ClOx and BrOx induced
56   ozone loss. *Tie and Brasseur* [1995] demonstrated that mid- and high latitude O_3 changes after a
57   volcanic eruption largely depend on chlorine loading. For the pre-industrial era and in the
58   absence of anthropogenic halogens in the stratosphere, O_3 would slightly increase in the middle
59   atmosphere after a large volcanic eruption resulting from the suppression of NOx-catalyzed
60   destruction by heterogenous creation of HNO_3 on volcanic aerosols. After the 1991 Pinatubo
61   eruption, the radiative heating caused by volcanic aerosols perturbed the local temperature and
62   circulation, which lifted the ozone layer and caused equatorial ozone depletion [*Kinnison et al.*,
63   1994]. *Wang et al.* [2022] reported that, in the case of the Hunga-Tonga eruption, mid-latitude
64   ozone reduction was primarily caused by anomalous upwelling. Enhanced water can also change
65   O_3. In the lower most stratosphere, H_2O injection through deep convection or tropopause cirrus
66   clouds could change the catalytic chlorine/bromine free-radical chemistry and shift the total
67   available inorganic chlorine towards the catalytically active free-radical form, ClO [*Solomon et*
68   *al.*, 1997; *Anderson et al.*, 2012].
69   *Evan et al.* [2023] report observations of decreased O_3 and HCl, and increased ClO in the
70   first week following the HTHH eruption at 20 hPa, which is related to the injected H_2O
71   exceeding the normal range of the stratospheric variability. Here we use the Whole Atmosphere
72   Community Climate Model version 6 (WACCM6) model [*Zhu et al.*, 2022] to analyze the
73   dynamic and chemical contributors to this initial in-plume ozone depletion, and to understand the
74   climate model performance. A lofting plume can bring ozone-poor tropospheric air into the
75   stratosphere and cause in-plume low ozone values compared with the surrounding stratospheric
76   air [*Yu et al.*, 2019]. For a submarine volcanic eruption, the in-plume air composition is not only
77   impacted by tropospheric air, but also by the seawater, and volcanic gases (including H_2O, CO_2,
78   SO_2, HCl, HF, H_2S, S_2, H_2, CO, and SiF_4.), and volcanic minerals. For the HTHH initial plume,
79   besides high H_2O and high SO_2, Microwave Limb Sounder (MLS) observations indicate the in-
80   plume air carried high CO (**Figure A1**), relatively low ozone, and high ClO, compared with the
81   surrounding air. We constrain the initial plume chemical compounds based on observational data
82   from MLS; then analyze how stratospheric chemistry changes the plume composition. We will
83   answer the following scientific questions:
84   1. What are the initial conditions in the volcanic plume?
85   2. What are the main causes of in-plume ozone depletion?
86   3. How do volcanic injections impact heterogeneous reactions that cause chlorine activation
87   in the plume?
88
89   **2. Observational data description and model setup**
90   The MLS instrument onboard the EOS Aura satellite was launched into a near-polar sun-
91   synchronous orbit in 2004. This work uses MLS version 4 for O_3, ClO, temperature, and CO data
92   during the first ten days after the eruption as recommended by *Millán et al.* [2022]. The vertical
93   resolution of these MLS products is typically around 3-5 km in the stratosphere. All data used
94   here were screened using the methodology indicated in *Livesey et al.* [2022]. We use the MLS

99 H$_2$O data to identify the plume location and define it as regions with water vapor larger than 10
100 ppmv.
101   *Vömel et al.* [2022] provide water vapor radiosonde measurements during the first three
102 global circumnavigations of the plume. Here we calculate the relative humidity relative to ice
103 (RHi) and compare the observed values with the simulated values.
104   We use the 70-layer WACCM model as described in *Zhu et al.* [2022], injecting SO$_2$
105 (0.42 Tg) and H$_2$O (150 Tg). The model has a horizontal resolution of 0.9° latitude × 1.25°
106 longitude. The injection plume in the model includes about 40 grid points. The model's vertical
107 resolution is about 1 km in the stratosphere. The model atmosphere is nudged to GEOS5
108 MERRA meteorological analysis [*Rienecker et al.,* 2008] until January 14, one day before the
109 eruption day. After January 15, we run the model freely with a fully interactive atmosphere and
110 ocean for ten days.
111   We constrain the simulated volcanic aerosol, H$_2$O, and chlorine by comparing to
112 observations during the first ten days after the eruption. *Zhu et al.* [2022] show that the simulated
113 aerosol backscatter coefficient agrees with the CALIPSO observations on January 17. The
114 simulated H$_2$O agrees with MLS [*Millán et al.*, 2022; *Zhu et al.*, 2022] from February 1 to April
115 1, 2022. Here, we compare the simulated H$_2$O with the radiosonde observations of humidity
116 [*Vömel et al.*, 2022] during the first week. **Figure 1** shows the RHi on January 18 and January 19
117 observed by the radiosonde and from nearby simulated model output. Both the observations and
118 simulations show relative humidity between 70% to 100%. The radiosonde observations have a
119 much higher vertical resolution than the model. Therefore, they show multiple layers of water
120 enhancement, while the model only shows one.
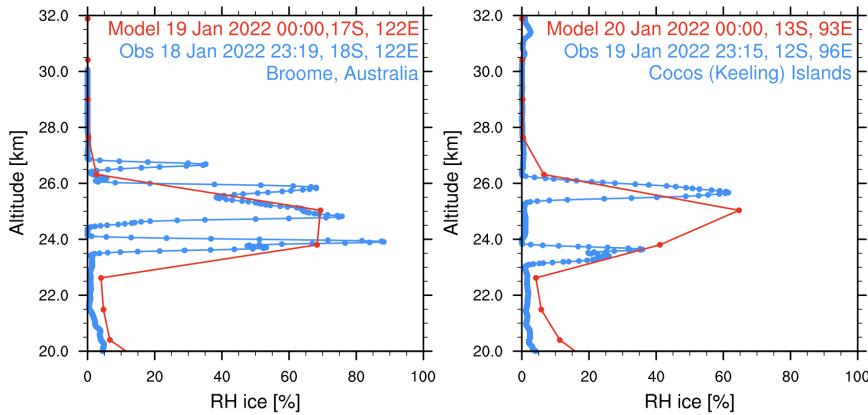
121
122 **Figure 1.** Relative humidity with respect to ice saturation vapor pressure from radiosondes (blue)
123 [*Vömel et al.*, 2022] and simulation (red). The profiles are picked at nearby locations. Note the
124 observations are about 45 minutes earlier in time than the simulations, which places them on a
125 different day.
126
127   We constrain the chlorine injection using MLS ClO observations at 20 hPa. **Figure 2a**
128 shows ClO from the MLS observations and the model simulations at 20 hPa from January 18 to
129 January 24. MLS values are selected from locations where water vapor is larger than 10 ppmv,
130 indicating these values are inside the volcanic plume. **Figures 2b** and **2c** show the simulated

133 daytime ClO for one plume location for each day. The dates are marked next to each plume.
134 MLS observations show elevated ClO, about 5 to 10 times higher than the ambient values
135 (**Figure 2a**). If we only inject SO_2 and H_2O (The H2O_SO2 case defined in Table 1), we get a
136 ClO amount about twice as large as the background (**Figure 2b**), which is much lower than
137 observed. The change of ClO indicates that H_2O alters the Cly partitioning. To match the
138 observed values, we need to inject 0.0013 Tg of ClO (**Figure 2c**). This is equivalent to injecting
139 ~0.0009 Tg of HCl (**Figure A2**). In our simulations, injecting ClO and HCl does not lead to
140 different HOCl (**Figure A3**), ClO, and O_3 levels after January 15, indicating the balancing of
141 ClO and HCl inside the HTHH plume happens very quickly. Unfortunately, the HOCl retrieval
142 from MLS is not suitable for scientific use at this pressure level, so we cannot validate it. We
143 choose the ClO injection case in our following analysis. Note that the MLS ClO vertical
144 resolution is ~2 km near 20 hPa, which is coarser than the model vertical resolution (~1 km at 20
145 hPa).
146
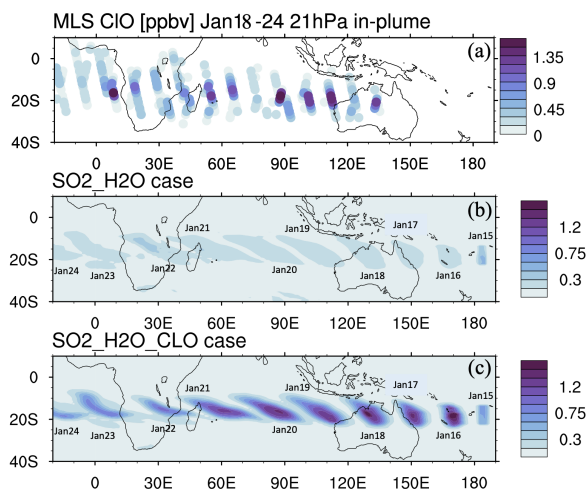
147
148 **Figure 2. a)** MLS in-plume ClO observations from January 18 - 24. "In-plume" is defined as the
149 area with water vapor mixing ratios larger than 10 ppmv. MLS in-plume ClO data is not
150 recommended for scientific use until January 18, 2022. **b)** and **c)** Simulated 10-day evolution of
151 in-plume ClO in the SO2_H2O and SO2_H2O_ClO case. The modeled ClO concentrations are
152 only taken during daytime each day (either 6 UTC or 12 UTC).

153
154   To investigate the O_3 decrease and its related chemical evolution during the first 10 days,
155 we conduct several simulations as described in **Table 1**.
156
157 **Table 1.** Model cases description.

Name	Description
Nonvolc	No injection of volcanic H_2O and SO_2.
H2O_SO2	H_2O and SO_2 injection profile follows Zhu et al. [2022].

H2O_SO2_ClO	Besides H_2O and SO_2, injection of 0.00013 Tg of ClO. ClO injection profile is proportional to H_2O injection.
H2O_SO2_ClO_nohet	Same setting as H2O_SO2_ClO, but turn off the heterogeneous chemical reactions for $HCl+HOCl$, $ClONO_2+H_2O$, and $ClONO_2+HCl$
SO2_ClO	SO_2 injection profile follows Zhu et al. (2022). No water injected. Injection of 0.00013 Tg of ClO using the same profile as H2O_SO2_ClO.
lowO3	Reduce the O_3 to 75% of its original value at 20 hPa.
H2O_SO2_lowO3	H_2O and SO_2 injection, plus reducing O_3 to 75%.
H2O_SO2_ClO_lowO3	H_2O, SO_2 and ClO injection, plus reducing O_3 to 75%.
H2O_SO2_NO	Injection of 0.003 Tg of NO in addition to H_2O and SO_2.

3. Results

Evan et al. [2023] show the HTHH in-plume ozone depletion at 20 hPa lasts at least ten days after the HTHH eruption, which they attribute to the heterogeneous chlorine activation on humidified volcanic aerosols. Here we analyze the contributions to this initial in-plume O_3 depletion considering three processes: 1) increasing H_2O injection may enhance the HOx catalytic cycle and HOx/ClOx interactions; 2) increasing ClO during the injection phase may deplete ozone due to both heterogeneous reactions and gas phase reactions; 3) the rising plume from the troposphere may carry ozone-poor tropospheric air into the stratosphere.

MLS observed in-plume low ozone concentration at 20 hPa (**Figure 3a**), especially during these three days: ozone concentrations of 4.8 ppmv on January 17, 4.6 ppmv on January 20, and 5.1 ppmv on January 24. These are ozone anomalies of about 1.7 ppmv, 1.9 ppmv, and 1.4 ppmv, respectively. The anomalies are calculated using the background average values in this area (6.5 ppmv) subtracting the low ozone values. Note that any interpretation of these O_3 anomalies needs to consider the coarse MLS vertical resolution (~3 km). Because the plume is spatially small during the initial days, MLS tracks do not capture the maximum plume perturbation every day. The simulation with the water injection (**Figure 3b**) accelerates the HOx catalytic cycle and shows evident O_3 reduction, but less than observed. Once we inject ClO on top of the massive water injection (**Figure 3c**), O_3 loss is significantly enhanced and is close to the observations after January 18. The difference between **Figure 3d** and **Figure 3c** is caused by heterogeneous reactions, which usually only happen in the stratospheric polar springtime where they cause the Antarctic ozone hole and Arctic ozone depletion. Heterogeneous reactions become important, despite the high non-polar temperatures because of the massive quantity of water injected. The heterogeneous reaction rate is strongly related to the relative humidity [Shi et al., 2001]. Usually, during the polar night, the relative humidity is higher (RHi 60%-100%) than in the non-polar stratosphere because of the low temperature (<195 K). Here, the water injection increases the relative humidity (**Figure 4c**). Enhanced water causes the weight percent of H_2SO_4 of the sulfuric acid aerosol to decrease from 70% to 35% (**Figure 4b**). The massive water injection also causes the in-plume temperature to drop about 2 to 6 K (**Figure 4f**) [Solomon et al., 2016]. All these factors (temperature decrease, relative humidity increase, and particle H_2SO_4 dilution) can increase the three heterogeneous reaction probabilities ($HCl+HOCl$, $ClONO_2+H_2O$, and $ClONO_2+HCl$). As shown in **Figure 5**, when the water vapor amount is near the

Moved down [1]: Figure 3d uses the same injection as **Figure 3c** but with heterogeneous reactions (i.e., $HCl+HOCl$, $ClONO_2+H_2O$, and $ClONO_2+HCl$) turned off.

206 climatological value of 6 ppmv, the heterogeneous reaction probability reaches 10^{-2} to 10^{-1} when
207 the temperature is ~190 K. Meanwhile, the reaction probability is similar for temperatures of 215
208 K when the water vapor is ~600 ppmv in the simulations, as was the case for the HTHH plume
209 during the week following the eruption. COSMIC-2 radio occultation observed even higher
210 water vapor during the first week: the maximum values over January 20-22 are ~1000-2000
211 ppmv [*Randel et al.,* 2023]. Also, because the in-plume and the out-of-plume chemical
212 concentrations are different, we apply both conditions (solid and dashed lines) to show how the
213 different HCl, HOCl, and ClONO$_2$ conditions alter the HCl+HOCl and ClONO$_2$+HCl reactions
214 probabilities by one order of magnitude. Volcanic sulfur injection also increases the sulfate
215 surface area density (**Figure 4a**) that provides extra surfaces for heterogeneous reactions.
216 Comparing **Figure 3b** and **3c** with MLS observations, we can see that the chemical
217 reactions do not explain the O$_3$ loss during the first three days of the eruption (January 15 -
218 January 17, low O$_3$ near 160˚E in MLS observation). This discrepancy suggests that the plume
219 contains some ozone-poor tropospheric air after the injection into the stratosphere. We ran three
220 cases with initial low ozone. For the low O$_3$ case (**Figure 3e**), we inject only ozone-poor air
221 without volcanic H$_2$O and SO$_2$. It shows low O$_3$ as observed during the first couple of days, but
222 ozone recovers quickly because the O$_3$ chemical lifetime is short at 20 hPa inside the plume
223 (**Figure A4**). The H2O_SO2_lowO3 case (**Figure 3f**) shows ozone loss similar to the
224 observation in the first six or seven days. By adding the ClO and initial ozone-poor air (**Figure**
225 **3g**), we obtain persistent low O$_3$ values that agree with the observational lowest values better
226 than the other cases (**Figure 6a**). Compared with **Figure 3b**, **Figure 3d** has slightly more ozone
227 depletion, indicating that the extra chlorine injection impacts O$_3$ even without heterogeneous
228 chemistry. However, without including the high amounts of injected water, the additional ClO
229 alone cannot deplete ozone much (**Figure 3h**).
230
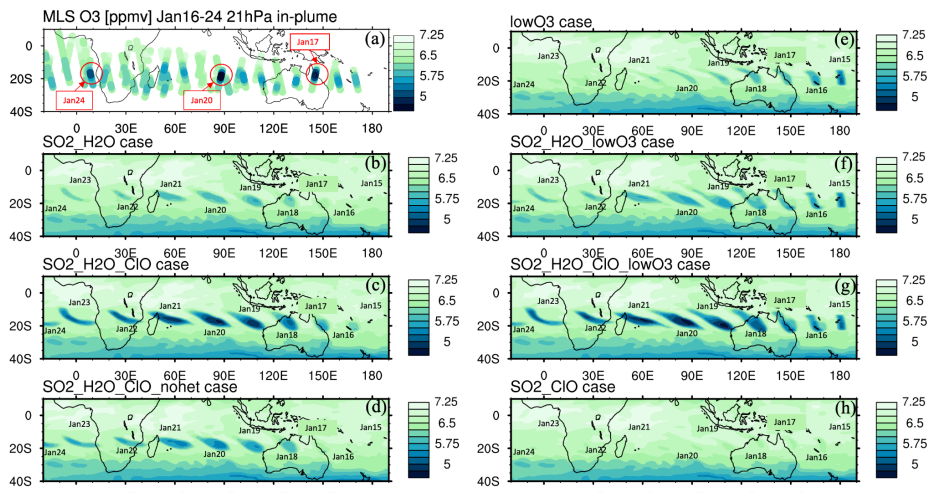
232 **Figure 3. a)** MLS in-plume O$_3$ observation from January 16 - 24. "In-plume" is defined as in
233 Figure 2. Note that MLS ozone retrievals were unaffected by the plume leading to the addition of
234 two extra days of data for this figure. The locations and days with low O$_3$ values used in **Figure**

237 **6** are marked with circles. **b–h)** Simulated 10-day evolution of in-plume O_3 in seven model cases
238 with various injections of SO_2, H_2O, ClO, and low initial O_3. **Figure 3d** uses the same injection
239 as **Figure 3c** but with heterogeneous reactions (i.e., $HCl+HOCl$, $ClONO_2+H_2O$, and
240 $ClONO_2+HCl$) turned off. The simulated O_3 in the H2O_SO2 case uses one model time step
241 each day that occurs near local noon.

242
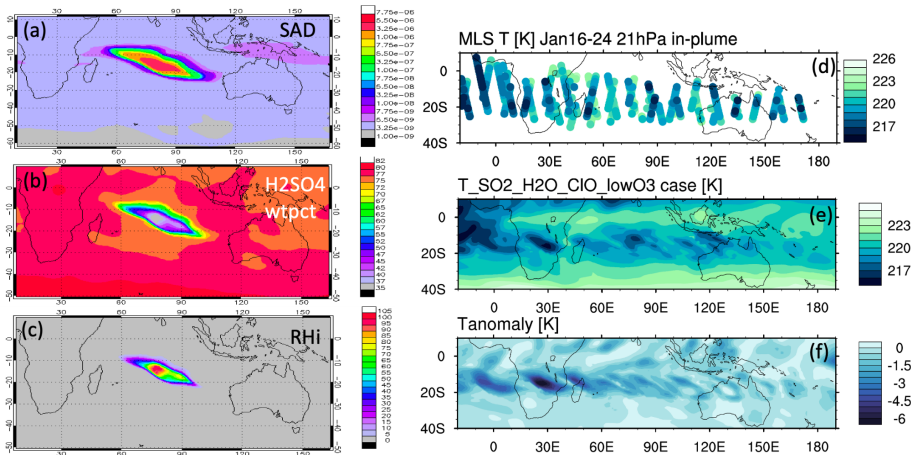
243
244 **Figure 4. a)** Simulated surface area density, **b)** simulated H_2SO_4/H_2O weight percent and **c)**
245 relative humidity on January 20 at 20 hPa. **d)** Temperature evolution during the first ten days at
246 20 hPa from MLS, **e)** simulated temperature evolution in the SO2_H2O_ClO_lowO3 case; **f)**
247 temperature difference between the SO2_H2O_ClO_lowO3 case and the Nonvolc case.

248
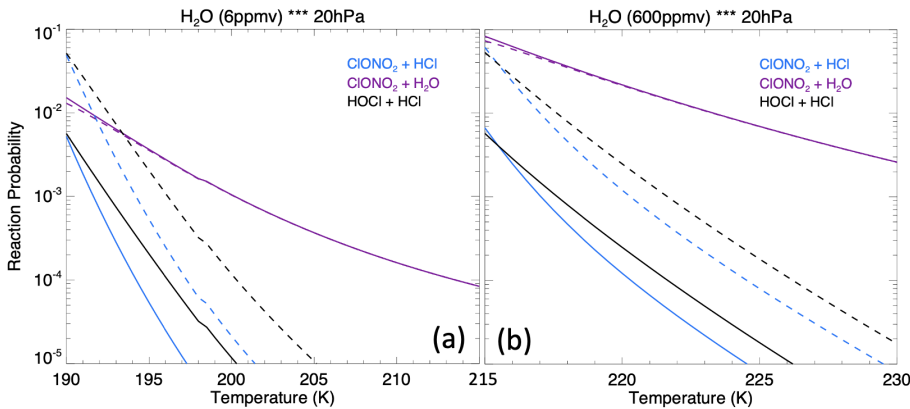
249
250 **Figure 5.** The heterogeneous reaction probability for three reactions on sulfate surfaces
251 ($ClONO_2+HCl$, $ClONO_2+H_2O$ and $HOCl+HCl$) as a function of water vapor assuming 0.4 µm
252 particle size at 20 hPa. Panel **a)** assumes 6 ppmv of ambient water vapor and panel **b)** assumes

600 ppmv of ambient water vapor. The solid lines use the out-of-plume chemical concentration on January 20: 1.0 ppbv of HCl, 0.03 ppbv of HOCl, and 0.5 ppbv of $ClONO_2$; the dashed lines use the in-plume chemical concentration: 0.1 ppbv of HCl, 1.0 ppbv of HOCl, and 0.05 ppbv of $ClONO_2$. These values are based on the simulation output.

Figure 6 shows the O_3 anomaly evolution from several model cases (**a**) and percentage contributions to the total ozone loss (**b, c**). The model case with all injections (initial low O_3, high H_2O, and high ClO) agrees well with MLS observations on the three days with the lowest O_3 values (**Figure 6a**). In **Figure 6b** and **6c**, the black bars represent the contribution from the low O_3 injection, which is significant during the first couple of days but diminishes quickly. From these percentage values, we conclude that the low O_3 carried in the plume lofting cannot be the reason for the low O_3 values after 3 days. Chemistry is the main reason that this O_3 depletion lasts so long.

There are two ways to look at the chemical contributors to ozone loss based on our model runs. The first is to separate the contributors due to various injections (**Figure 6c**): H_2O injection accounts for about 30-40% of the ozone loss most of the time (blue) and ClO injection accounts for 50% of the ozone loss most of the time (red). However, we cannot simply attribute the largest contribution to the ClO injection, because if we only inject ClO, it does not produce much ozone depletion (**Figure 6a,** magenta). It is the ClOx/HOx interactions that accelerate O_3 depletion.

A second way to look at the causes for ozone loss is to separate the contributions from the gas-phase chemistry and the heterogeneous chemistry (**Figure 6b**). The model run with the H_2O and ClO injections, but without the heterogeneous chemistry shows that the gas-phase chemistry (yellow bars) account for more than 47% of the ozone loss from January 18 - 24. Heterogeneous chemistry (green bars) destroys about 30% of the ozone. Hence, both heterogeneous chemistry and gas-phase chemistry are important for O_3 depletion. Once we turn off the heterogeneous chemistry, the partitioning between active chlorine and chlorine in the reservoirs is changed. The order in which the processes are accounted for can affect the resulting breakdown. Thus, we cannot simply say that gas phase chemistry contributions are larger than heterogeneous chemistry. Both are clearly significant.
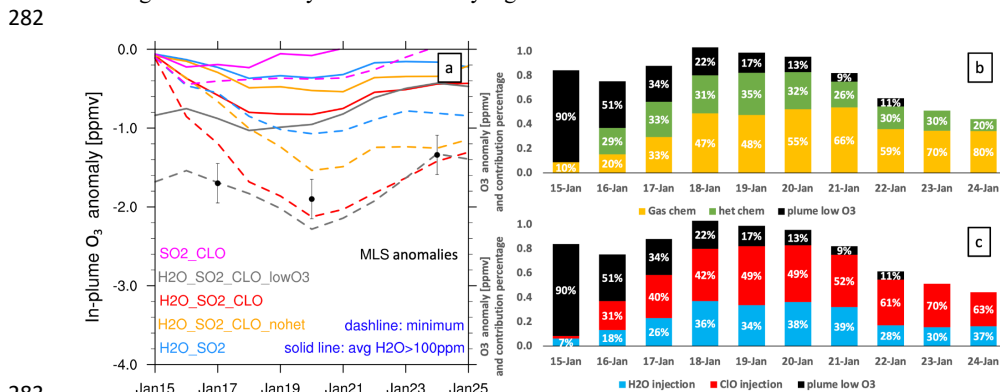
Figure 6. a) O_3 anomaly in different model cases. The solid lines are the average O_3 anomaly at 20 hPa on each day near local noon where water vapor is larger than 100 ppmv. 100 ppmv here is suggested by *Evan et al.* [2023], who found that O_3 anomalies are not significant for a 10

287 ppmv but significant for a 100 ppmv threshold. The dashed lines are the simulated maximum O_3
288 anomaly on each day at 20 hPa. The black dots show the three days during which MLS measures
289 the lowest O_3 values (explained in **Figure 3a**). **b)** The percentage contributions to ozone loss
290 from gas phase chemistry (orange) (H2O_SO2_CLO_nohet), heterogeneous chemistry (green,
291 H2O_SO2_CLO minus H2O_SO2_CLO_nohet), and low O_3 air carried into the stratosphere
292 (black, H2O_SO2_CLO_lowO3 minus H2O_SO2_CLO). **c)** The percentage contributions to
293 ozone loss from H_2O injection (blue, H2O_SO2 minus Nonvolc), ClO injection (red,
294 H2O_SO2_CLO minus H2O_SO2), and low O_3 air carried into the stratosphere (black,
295 H2O_SO2_CLO_lowO3 minus H2O_SO2_CLO).
296
297   To better understand which reactions are critical in the HTHH plume, we investigate the
298 simulated reaction rates related to HOx and chlorine compounds (**Figure 7**). These reactions
299 reflect how the water and ClO injections strengthen the in-plume HOx/ClOx interactions,
300 chlorine activation, and the relative importance of each heterogeneous reaction rate. The
301 WACCM model uses the methods developed by *Shi et al.* [2001] for heterogeneous reaction rate
302 calculations. **Figure 7a** shows the HOx cycle inside and outside the water plume on Januray 20,
303 daytime, at 20 hPa. The HO_2+O_3 reaction rate increases by a factor of four (from $5x10^4$ to $2x10^5$
304 $cm^{-3}sec^{-1}$); OH+O increases by a factor of ~four (from $2x10^4$ to $7.5x10^4$ $cm^{-3}sec^{-1}$; HO_2+O
305 increases by a factor of four (from $2x10^4$ to $8x10^4$ $cm^{-3}sec^{-1}$). In addition, the extra HOx plays a
306 large role in chlorine activation. **Figure 7b** shows the chlorine compound reactions inside the
307 HTHH initial plume. The HOCl photolysis rate increases by a factor of ~30 inside the plume
308 (from $6x10^3$ $cm^{-3}sec^{-1}$ outside the plume to $2x10^5$ $cm^{-3}sec^{-1}$) due to the high HOCl mixing ratio,
309 which is the dominant process causing the increase in chlorine activation to Cl. The HOCl
310 concentration remains high due to the enhanced ClOx/HOx interaction (i.e.,
311 $ClO+HO_2 \rightarrow HOCl+O_2$ reaction), as well as the increase of the heterogeneous reaction rate of
312 $ClONO_2+H_2O$ by five orders of magnitude (from 0.3 to $1x10^4$ $cm^{-3}sec^{-1}$). The large amounts of
313 HOCl also make the heterogeneous reaction of HOCl+HCl faster than the $ClONO_2+HCl$
314 reaction, while the latter reaction is known as the major reaction contributing to the chlorine
315 activation that contributes to the polar ozone depletion. **Figure A5** shows the uptake coefficient
316 for the three heterogeneous reactions HCl+HOCl, $ClONO_2+H_2O$, and $ClONO_2+HCl$ on January
317 20. The reaction probability of $ClONO_2+HCl$ is increased by eight orders of magnitude (from the
318 background value of 10^{-10} to 10^{-2}). This value is even higher than *Evan et al.* [2023] suggested,
319 who estimate that enhanced water increases the uptake coefficient of $ClONO_2+HCl$ to 10^{-4} cm^{-}
320 $^3sec^{-1}$. The reaction probability of HCl+HOCl and $ClONO_2+H_2O$ increases to 10^{-2}. Furthermore,
321 inside the plume, the reactions that convert Cl back to HCl are slower than their activation rate.
322   Besides the ozone loss reactions, ozone production reactions are also significantly altered
323 by the water plume (**Figure 7c**). HO_2+NO is usually not an important process for O_3 production
324 in the stratosphere (more important in the troposphere). The reaction rate doubles inside the
325 plume (from $1x10^5$ $cm^{-3}sec^{-1}$ to $2x10^5$ $cm^{-3}sec^{-1}$). Note that we don't inject lightning NOx in this
326 case, a possible scenario during the eruption phase, that can also further increase the O_3
327 production (detailed in the discussion section).
328   Comparing the partitioning of Cly
329 ($Cl+ClO+2Cl_2+2Cl_2O_2+OClO+HOCl+ClONO_2+HCl+BrCl$) reveals the in-plume chlorine
330 activation processes (**Figure 8**). Outside the plume, HCl and $ClONO_2$ are dominant, indicating
331 that most of the Cl is in reservoirs. While inside the water plume, both the H2O_SO2 and
332 H2O_SO2_ClO cases show strong depletion of the reservoirs HCl and $ClONO_2$, and most of the

355 Cly is either in the form of HOCl (a short-lived reservoir) or is activated in the form of ClO.
356 Unlike the chlorine activation process in the polar winter, HOCl is the highest in the HTHH
357 plume because heterogeneous chemistry is not fast enough to destroy HOCl to produce ClO. In
358 the case without heterogeneous chemistry, HCl and $ClONO_2$ are dominant in the plume,
359 indicating that heterogeneous chemistry is the main process of converting HCl to active chlorine.
360 Comparing total Cly and ClO in all panels, ClO does not exceed a quarter of the Cly, indicating
361 adding 0.00013Tg of ClO through injection is one way to produce the observed ClO. There is a
362 possibility that ClO is converted from other Cly species through chemical reactions we are not
363 aware of because this was a very unusual eruption.

364

365
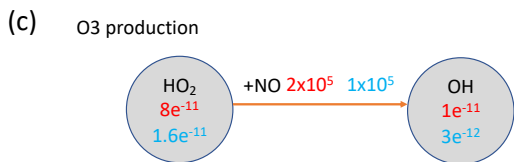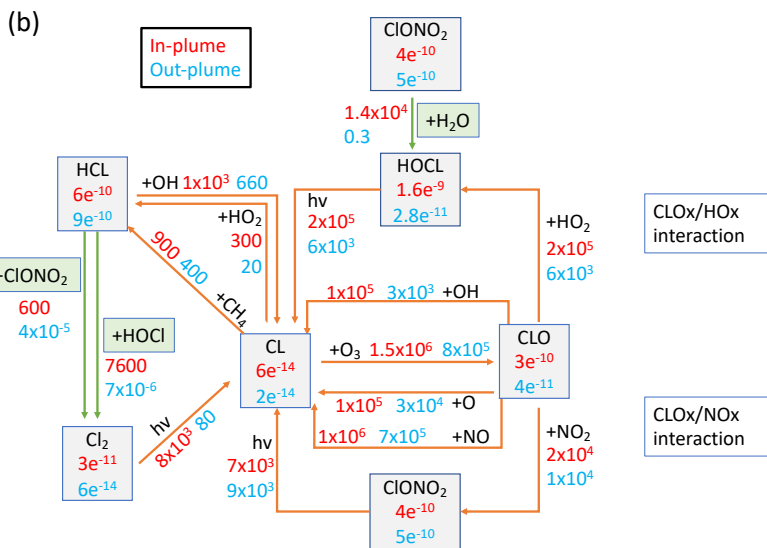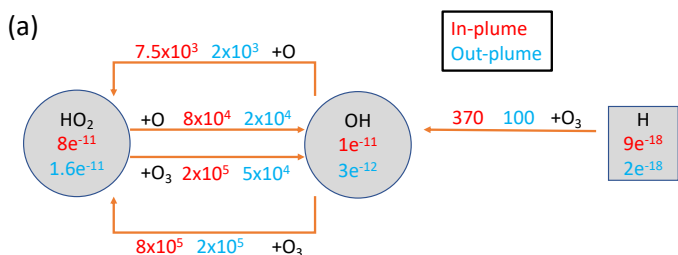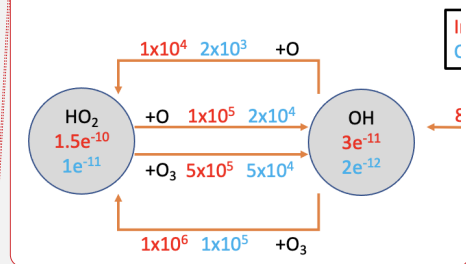
Figure 7. Reactions inside and outside the plume in $cm^{-3}sec^{-1}$ and compound concentrations in mol/mol. Red numbers represent values inside the plume, blue numbers outside the plume. **a)** HOx balance and its interaction with Ox during daytime at 20 hPa on January 20, 2022. **b)** Chlorine compound reactions in the H2O_SO2_ClO case. **c)** HOx cycle impact on O_3 production. Green arrows represent the heterogeneous reactions for chlorine activation. H_2O is ~ 600 ppm inside the plume and ~5.5 ppm outside the plume. Cly is ~ 4.2 ppbv inside the plume and 1.5 ppbv outside the plume.
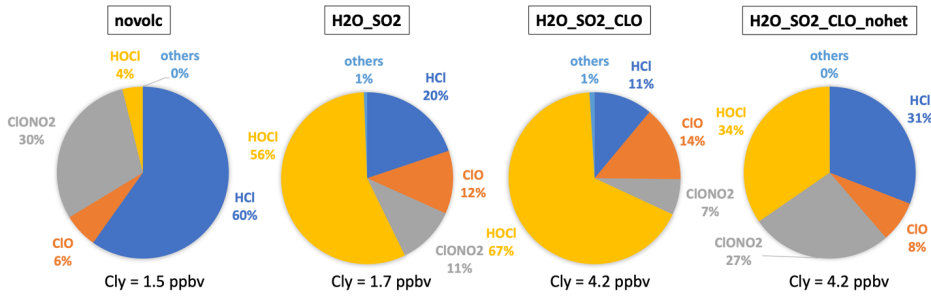
Figure 8. The percentage of each inorganic chlorine compound (Cly=Cl+ClO+$2Cl_2$+$2Cl_2O_2$+OClO+HOCl+$ClONO_2$+HCl+BrCl) inside and outside the plume. The slight difference between novolc Cly and H2O_SO2 Cly is because H_2O injection changes the plume dynamics in the free-running simulations.

4. Discussion

The ozone loss inside the HTHH plume during the first ten days provides a unique opportunity to study stratospheric chemistry and to understand the performance of the WACCM state-of-the-art climate model, because the HTHH injected ClO and H_2O exceed the normal range of the stratospheric variability. These volcanic injections strongly altered the ClOx/HOx interactions and heterogeneous reaction rates, producing different chemical pathways for chlorine activation and ozone depletion from what occurs in the Antarctic ozone hole or Arctic ozone depletion in the polar stratospheric winter and spring. HOCl is identified as playing a large role in the in-plume chlorine balance and heterogeneous processes. The high HOCl concentrations are a result of the very high in-plume water vapor content, which makes this event different from chemistry in the Antarctic ozone hole, where $ClONO_2$ is more important.

This study also raises an interesting question of where the Cl comes from in the volcanic injection. Seawater contains 3.5% sea salt, which implies that about 5 Tg of NaCl could have been injected assuming that the injected 150 Tg of H_2O came from sea water. However, we only need to inject 0.00013 Tg of ClO to match the MLS ClO observations during the first few days after the eruption. We also conducted a test injecting an equivalent amount of HCl (0.0009 Tg), which resulted in a similar HOCl, ClO, and O_3 pattern (**Figure A2 and A3**). If we inject more HCl or ClO, ClO would exceed the observed concentration, causing depletion of OH, and slowing down the SO_2 oxidation. Evidently, if the water came from seawater, most NaCl was not converted to HCl but stayed in the stratosphere as particles. *Vernier et al.* [2023] sampled NaCl particles eight months after the eruption near Brazil. Based on their sampled NaCl concentration, we estimate 0.5 to 1 Tg of NaCl may have been injected and stayed in the atmosphere. There are
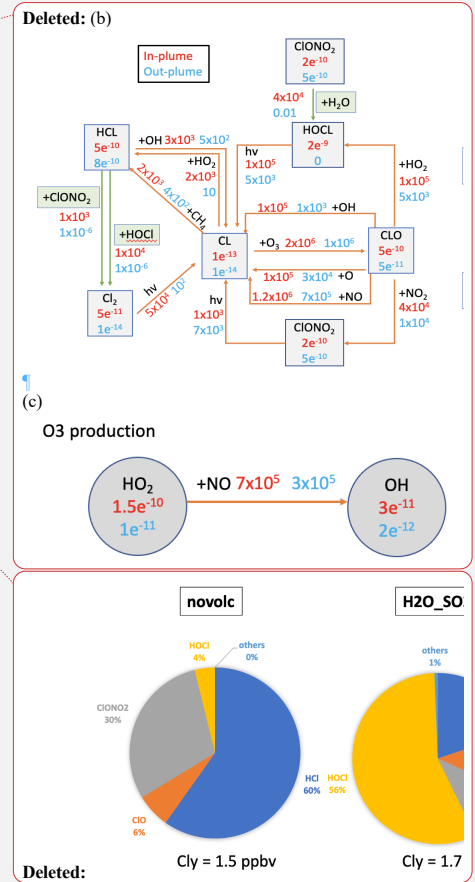
several possibilities why this event did not inject 5 Tg of NaCl in the stratosphere: Remote sensing particle size estimations [*Khaykin et al.*, 2022] and in-situ measurements [*Asher et al.,* 2023] indicates that the particles were submicron sized. However, sea salt particles injected into the lower troposphere by wind are mainly particles larger than 10 µm. Hence, if the volcanic injection had similar sized NaCl particles, most of them may have quickly fallen out of the stratosphere. In addition, the majority of NaCl might have been washed out during the first couple of hours of plume injection by acting as nuclei for ice particles. It is also possible that the reactions that might release Cl from NaCl may not efficiently lead to reactive Cl. For example, HNO_3 can react on sea salt heterogeneously very quickly in the troposphere to release HCl (De Haan and Finlayson-Pitts, 1997; Guimbaud et al., 2002; Murphy et al., 2019). This reaction may be accelerated by HTHH high humidity even if the temperature is low in the stratosphere. HCl could be removed by condensing in supercooled water, which would reduce HCl vapor concentrations by up to four orders of magnitude, preventing substantial stratospheric chlorine injection [*Tabazadeh and Turco*, 1993]. Finally, it may be that the water injected came from magmatic water, or seawater that percolated into the volcano and was released as steam. Such water would not be rich in NaCl. In that case Cl observed by *Vernier et al.* [2023] may have been bound up in minerals of the volcanic ash. Other halogen species such as bromine and iodine are often observed after volcanic eruptions (large amounts of BrO were observed after HTHH in the troposphere [*Li et al.,* 2023]). However, they can lead to much stronger ozone depletion if they persist in the stratosphere. Since the elevated Cl in the model can well explain the O_3 depletion, the impact of bromine and iodine on stratospheric O_3 is minimal for this eruption.

In addition, NOx can be produced by lighting inside or around the volcanic plume. Observations show there was a record number of lightning events in this volcanic plume. Almost 400,000 flashes were observed by the GLD360 network over the 6 hours of the most active eruption period (and ~590,000 total flashes) [Global Volcanism Program, 2022]. Considering that tropospheric global models use a lightning source of 5 Tg(N)/yr and an average flash the OTD/LIS satellite sensors produced an average global flash rate of 44±5 flashes per second, an injection of N of ~0.001- 0.003 Tg (0.002 - 0.006 Tg of NO) would be expected for the HTHH eruption. We conducted a model run with H_2O, SO_2, and an injection of 0.003 Tg of NO (the H2O_SO2_NO case), showing that this additional NO has little impact on the O_3 loss and ClO levels during the first ten days (**Figure A6**). Compared to the H2O_SO2 case, the simulated O_3 loss in the H2O_SO2_NO case increased by ~ $5x10^5$ molecules/cm^3/sec, but at the same time, the O_3 production rate increased by ~ $5x10^5$ molecules/cm^3/sec. The $NO+HO_2$ reaction rate in the H2O_SO2_NO case increases 5 times compared with the H2O_SO2 case. Therefore, lighting NOx probably does not contribute to the HTHH initial in-plume O_3 loss. Because of the high water, NO would convert to HNO_3 in the first couple of days. Unfortunately, we lack observations of HNO_3, NO, or NO_2 right after the eruption. MLS observations in February (**Figure A7**) and the model simulations with H_2O injection or H_2O+NO injections show elevated HNO_3 compared with the background.

Appendix A

455
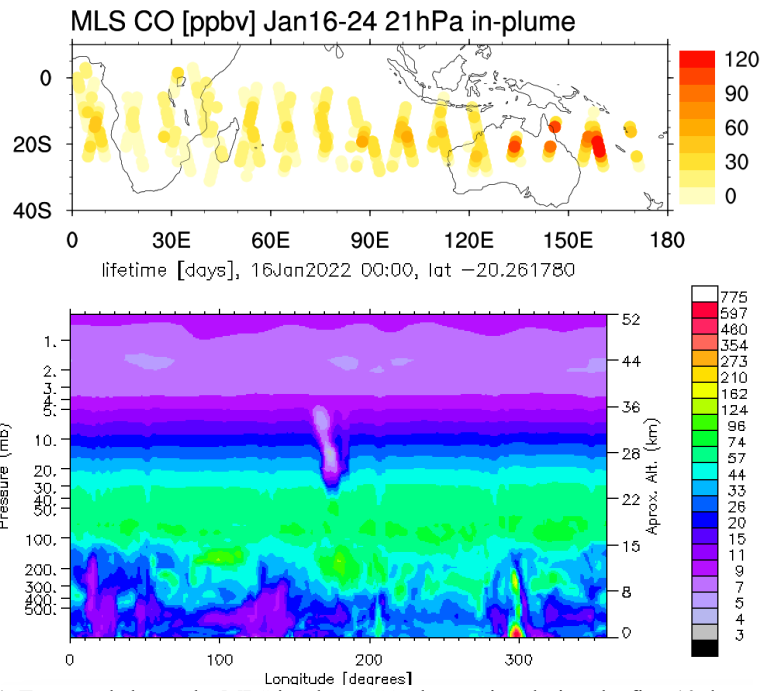
456
457 **Figure A1.** Top panel shows the MLS in-plume CO observation during the first 10 days after the
458 eruption. The bottom panel shows the CO lifetime on Jan 16 at 20°S is shortened from a month
459 to a few days because of the volcanic water plume. The observed CO mixing ratios of around
460 120 ppmv seem incompatible with typical CO levels over oceanic regions, indicating the
461 production of CO within the magma chamber or in the hot plume itself.
462
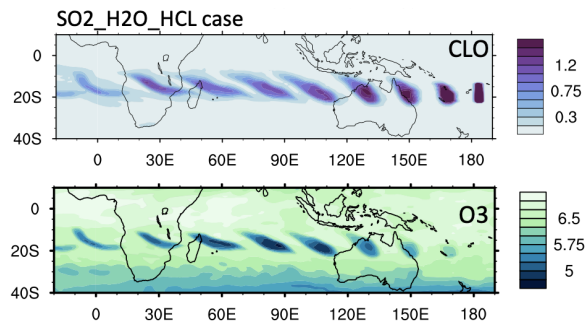
463
464 **Figure A2.** The O_3 and ClO evolution from the model case with an HCl injection of 0.000092
465 Tg (equivalent to 0.00013 Tg of ClO injection).
466
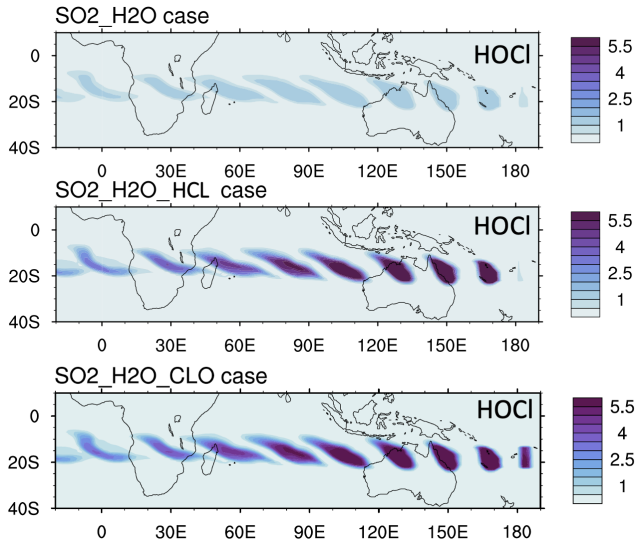
467
468 **Figure A3.** The HOCl evolution from the three model cases.
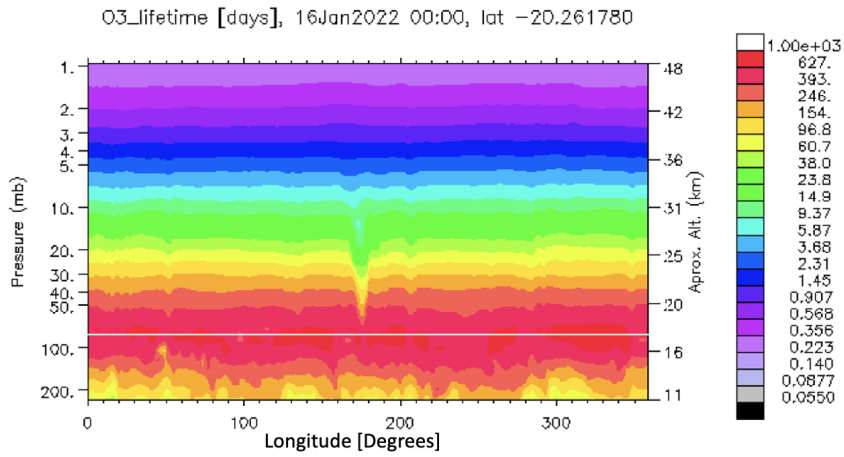
469
470 **Figure A4.** O_3 chemical lifetime is about 1 to 2 months at 20 hPa and is reduced to 10 days at the
471 HTHH location.
472
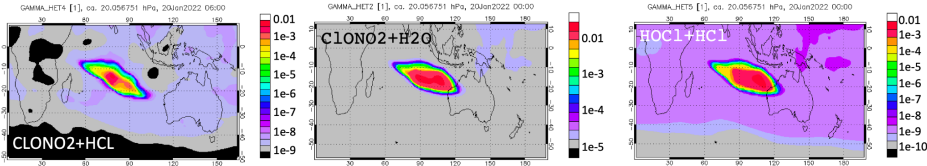
473
474 **Figure A5.** Heterogeneous reaction probabilities for the three heterogeneous reactions on
475 January 20 at 20 hPa.
476
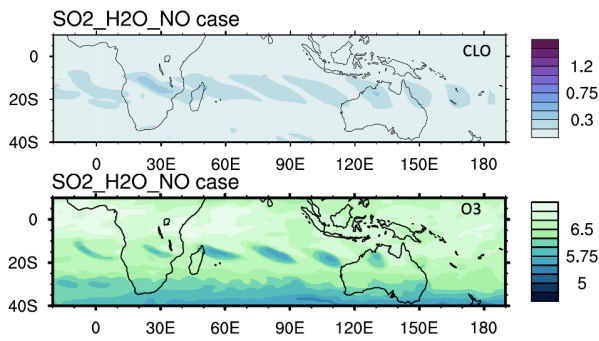
477
478
479 **Figure A6.** O_3 and ClO evolution from the model case with NO injection of 0.003 Tg, which is
480 identical to the SO2_H2O case. The ClO and O_3 enhancement are due to the H_2O injection.

481
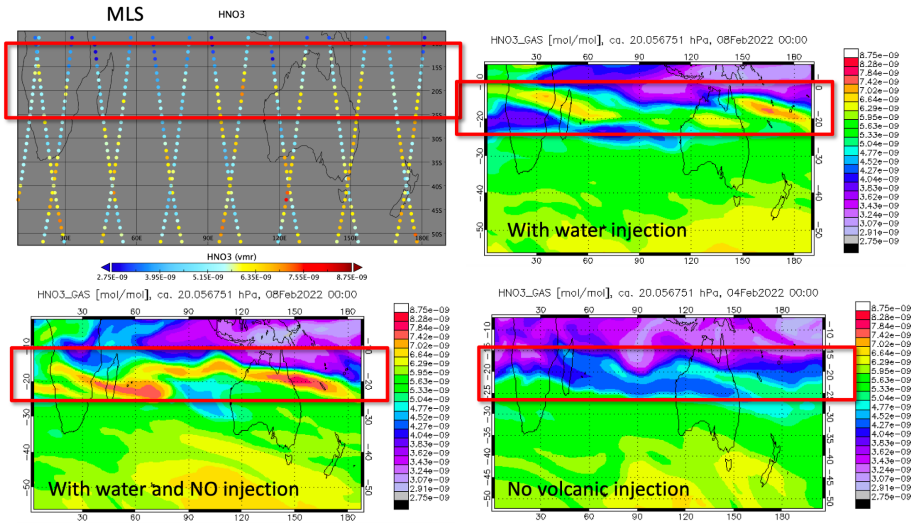
Figure A7. HNO_3 observed by MLS on February 8, 2022 compared to the model simulation with water and NO injection, as well as the no volcanic injection case. MLS shows similar elevated HNO_3 as the simulation case with H_2O injection or with H_2O/NO injection.

Code availability: The CESM2 model is available on the CESM trunk to any registered user at www.cesm.ucar.edu.

Data availability: The main simulation data generated during this study are available at (https://osf.io/f69ns/) with a permanent DOI 10.17605/OSF.IO/F69NS. Aura MLS v4 data is available at https://disc.gsfc.nasa.gov/datasets?page=1&keywords=AURA%20MLS. Water vapor radiosonde data is available at https://doi.org/10.5065/p328-z959 (26).

Author contribution: YZ, RWP, DK, and KHR designed the experiments and YZ performed the simulations. YZ prepared the manuscript with contributions from all co-authors. DK examined the sensitivity of the stratospheric H_2O abundance on the reaction probability (Figure 5). LM, HV and SE provided observational data and analysis. RWP, DK, OBT, JZ, ST, CGB, XW, WJR and KHR participated in the modeling data analysis.

Competing interests: At least one of the (co-)authors is a member of the editorial board of Atmospheric Chemistry and Physics.

Acknowledgement

This project received funding from NOAA's Earth Radiation Budget (ERB) Initiative (CPO #03-01-07-001). This research was supported in part by NOAA cooperative agreements NA17OAR4320101 and NA22OAR4320151. We thank Hazel Vernier, Dr. Kimberlee Dube, Dr. Pengfei Yu, Fracis Vitt, Dr. Ru-shan Gao, Dr. Margaret Tolbert, Dr. Micheal Mills, Dr. Daniel Murphy, and Dr. Brian Ridley for their valuable input. NCAR's Community Earth System Model project is supported primarily by the National Science Foundation. This material is based upon work supported by the National Center for Atmospheric Research, which is a major facility sponsored by the NSF under Cooperative Agreement No. 1852977. Computing and data storage resources, including the Cheyenne supercomputer (doi:10.5065/D6RX99HX), were provided by the Computational and Information Systems Laboratory (CISL) at NCAR. Work at the Jet Propulsion Laboratory, California Institute of Technology, was carried out under a contract with the National Aeronautics and Space Administration (80NM0018D0004).

Reference:

519 Anderson, J. G., D. M. Wilmouth, J. B. Smith, and D. S. Sayres (2012), UV Dosage Levels in
520   Summer: Increased Risk of Ozone Loss from Convectively Injected Water Vapor, *Science*,
521   *337*(6096), 835-839, doi: https://doi.org/10.1126/science.1222978.
522 Asher, E., Todt, M., Rosenlof, K.H., Thornberry, T.D., Gao, R.S., Taha, G., Walter, P.J.,
523   Alvarez, S.L., Flynn, J., Davis, S.M. and Evan, S., (2022). The unprecedented rapid aerosol
524   formation from the Hunga Tonga-Hunga Haʹapai eruption. AGU Fall Meeting Abstracts
525   (Vol. 2022, pp. A42I-01).
526 De Haan, D. O.; Finlayson-Pitts, B. J. Knudsen cell studies of the reaction of gaseous nitric acid
527   with synthetic sea salt at 298 K. J. Phys. Chem. A 1997, 101, 9993-9999,
528   doi:10.1021/jp972450s.
529 Evan et al., (2023), Rapid ozone loss following humidification of the stratosphere by the Hunga
530   Tonga Eruption, accepted by Science.
531 Global Volcanism Program, 2022. Report on Hunga Tonga-Hunga Ha'apai (Tonga). In: Sennert,
532   S K (ed.), Weekly Volcanic Activity Report, 12 January-18 January 2022. Smithsonian
533   Institution and US Geological Survey.
534 Guimbaud, C.; Arens, F.; Gutzwiller, L.; Gäggeler, H. W.; Ammann, M. Uptake of HNO3 to
535   deliquescent sea-salt particles: a study using short-lived radioactive isotope tracer 13N.
536   Atmos. Chem. Phys. 2002, 2, 249-257, doi:10.5194/acp-2-249-2002.
537 Hofmann, D. J., and S. J. Oltmans (1993), Anomalous Antarctic ozone during 1992: Evidence
538   for Pinatubo volcanic aerosol effects, *Journal of Geophysical Research: Atmospheres*,
539   *98*(D10), 18555-18561, doi:https://doi.org/10.1029/93JD02092.
540 Khaykin, S., et al. (2022), Global perturbation of stratospheric water and aerosol burden by
541   Hunga eruption, *Communications Earth & Environment*, *3*(1), 316, doi:10.1038/s43247-022-
542   00652-x.
543 Kinnison, D. E., K. E. Grant, P. S. Connell, D. A. Rotman, and D. J. Wuebbles (1994), The
544   chemical and radiative effects of the Mount Pinatubo eruption, *Journal of Geophysical
545   Research: Atmospheres*, *99*(D12), 25705-25731, doi: https://doi.org/10.1029/94JD02318.
546 Li, Q., Qian, Y., Luo, Y., Cao, L., Zhou, H., Yang, T., ... & Liu, W. (2023). Diffusion Height and
547   Order of Sulfur Dioxide and Bromine Monoxide Plumes from the Hunga Tonga–Hunga
548   Ha'apai Volcanic Eruption. *Remote Sensing*, *15*(6), 1534.
549 Livesey, N., J., Read., W. G., Wagner, P. A., Froidevaux, L., Santee, M. L., Schwartz, M. J., et
550   al. (2022), Version 5.0x Level 2 and 3 data quality and description document (Tech. Rep.
551   No.JPL D-105336 Rev. B). Jet Propulsion Laboratory, Retrieved from
552   https://mls.jpl.nasa.gov/data/v5-0_data_quality_document.pdf
553 Millán, L., et al. (2022), The Hunga Tonga-Hunga Ha'apai Hydration of the Stratosphere,
554   *Geophysical Research Letters*, *49*(13), e2022GL099381,
555   doi:https://doi.org/10.1029/2022GL099381.
556 Murphy, D. M., Froyd, K. D., Bian, H., Brock, C. A., Dibb, J. E., DiGangi, J. P., ... & Yu, P.
557   (2019). The distribution of sea-salt aerosol in the global troposphere. *Atmospheric Chemistry
558   and Physics*, *19*(6), 4093-4104.
559 Portmann, R. W., S. Solomon, R. R. Garcia, L. W. Thomason, L. R. Poole, and M. P.
560   McCormick (1996), Role of aerosol variations in anthropogenic ozone depletion in the polar
561   regions, *Journal of Geophysical Research: Atmospheres*, *101*(D17), 22991-23006,
562   doi:https://doi.org/10.1029/96JD02608.

Randel, W. J., Johnston, B. R., Braun, J. J., Sokolovskiy, S., Vömel, H., Podglajen, A., & Legras, B. (2023). Stratospheric Water Vapor from the Hunga Tonga–Hunga Ha'apai Volcanic Eruption Deduced from COSMIC-2 Radio Occultation. *Remote Sensing*, *15*(8), 2167.

Rienecker, M. M. et al. The GEOS-5 Data Assimilation System: Documentation of Versions 5.0. 1, 5.1. 0, and 5.2. 0 (2008).

Shi, Q., J. T. Jayne, C. E. Kolb, D. R. Worsnop, and P. Davidovits (2001), Kinetic model for reaction of ClONO2 with H2O and HCl and HOCl with HCl in sulfuric acid solutions, *Journal of Geophysical Research: Atmospheres*, *106*(D20), 24259-24274, doi:https://doi.org/10.1029/2000JD000181.

Solomon, S., S. Borrmann, R. R. Garcia, R. Portmann, L. Thomason, L. R. Poole, D. Winker, and M. P. McCormick (1997), Heterogeneous chlorine chemistry in the tropopause region, *Journal of Geophysical Research: Atmospheres*, *102*(D17), 21411-21429, doi:https://doi.org/10.1029/97JD01525.

Solomon, S., D. J. Ivy, D. Kinnison, M. J. Mills, R. R. Neely, and A. Schmidt (2016), Emergence of healing in the Antarctic ozone layer, *Science*, *353*(6296), 269-274, doi:https://doi.org/10.1126/science.aae0061.

Solomon, S., Rosenlof, K.H., Portmann, R.W., Daniel, J.S., Davis, S.M., Sanford, T.J. and Plattner, G.K., 2010. Contributions of stratospheric water vapor to decadal changes in the rate of global warming. Science, 327(5970), pp.1219-1223. DOI:10.1126/science.1182488

Tabazadeh, A., and R. P. Turco (1993), Stratospheric Chlorine Injection by Volcanic Eruptions: HCl Scavenging and Implications for Ozone, *Science*, *260*(5111), 1082-1086, doi: https://doi.org/10.1126/science.260.5111.1082.

Tie, X., and G. Brasseur (1995), The response of stratospheric ozone to volcanic eruptions: Sensitivity to atmospheric chlorine loading, *Geophysical Research Letters*, *22*(22), 3035-3038, doi:https://doi.org/10.1029/95GL03057.

Vernier, H., Quintão, D., Biazon, B., Landulfo, E., Souza, G., J. S. Lopes, F., Rastogi, N., Meena, R., Liu, H., Fadnavis, S., Mau, J., K. Pandit, A., Berthet, G., and Vernier, J.-P.: Understanding the impact of Hunga-Tonga undersea eruption on the stratospheric aerosol population using Balloon measurements, Satellite data, and model simulations, EGU General Assembly 2023, Vienna, Austria, 24–28 Apr 2023, EGU23-6882, https://doi.org/10.5194/egusphere-egu23-6882, 2023.

Vömel, H., S. Evan, and M. Tully (2022), Water vapor injection into the stratosphere by Hunga Tonga-Hunga Ha'apai, *Science*, *377*(6613), 1444-1447, doi: https:/doi.org/10.1126/science.abq2299.

Wang, X., W. Randel, Y. Zhu, S. Tilmes, J. Starr, W. Yu, R. Garcia, B. Toon, M. Park, and D. Kinnison (2022), Stratospheric climate anomalies and ozone loss caused by the Hunga Tonga volcanic eruption, *Authorea Preprints*.

Yu, P., et al. (2019), Black carbon lofts wildfire smoke high into the stratosphere to form a persistent plume, *Science*, *365*(6453), 587-590, doi:https://doi.org/10.1126/science.aax1748.

Zhu, Y., et al. (2022), Perturbations in stratospheric aerosol evolution due to the water-rich plume of the 2022 Hunga-Tonga eruption, *Communications Earth & Environment*, *3*(1), 248, doi:10.1038/s43247-022-00580-w.